Regional Land–Atmosphere Interactions in Southern Africa: Potential Impact and Sensitivity of Forest and Plantation Change

10

Zhenyu Zhang ⓘ, Patrick Laux ⓘ, Jussi Baade ⓘ, Hassane Moutahir ⓘ, and Harald Kunstmann ⓘ

Abstract

Southern Africa is experiencing increasing land transformation and natural vegetation losses. Deforestation is one type of this land degradation where there are indigenous forests present, and afforestation of other nature ecosystems with timber plantations. This study performs regional coupled land–atmosphere model simulations using the Weather Research and Forecast (WRF) model with a resolution of 12 km, to assess the impact of forest and plantation cover change on regional climate in southern Africa. Three WRF simulations were designed for different land covers: (i) MODIS-derived land cover for the year 2000 (baseline), (ii) Landsat-based forest and plantation change map during 2000–2015 overlain on the baseline and (iii) theoretical forest and plantations removal relative to the baseline. Modeling results suggest that conversion of forest and plantations

Z. Zhang (✉) · P. Laux · H. Kunstmann
Institute of Geography, University of Augsburg, Augsburg, Germany

Institute of Meteorology and Climate Research (IMK-IFU), Karlsruhe Institute of Technology, Campus Alpin, Garmisch-Partenkirchen, Germany
e-mail: zhenyu.zhang@kit.edu; zhenyu.zhang@partner.kit.edu; patrick.laux@kit.edu; harald.kunstmann@kit.edu

J. Baade
Department for Physical Geography, Friedrich-Schiller-University, Jena, Germany
e-mail: jussi.baade@uni-jena.de

H. Moutahir
Institute of Meteorology and Climate Research (IMK-IFU), Karlsruhe Institute of Technology, Campus Alpin, Garmisch-Partenkirchen, Germany

The Mediterranean Center for Environmental Studies (CEAM), Valencia, Spain
e-mail: hassane.moutahir@kit.edu

landscape to croplands and sparse vegetated land may result in a warmer and drier local climate, increasing daytime temperature by up to 0.6°C during the austral summer, and regulation of energy exchanges by decreasing the latent heat flux. In addition, results suggest that the removal of forest cover in northern part of southern Africa may decrease local precipitation recycling by around 1.2%. While the benefits of conserving native forests are obvious from an ecological perspective, afforestation considerations still require more detailed and local-scale treatments along the soil–vegetation–atmosphere continuum.

10.1 Introduction

Forests cover more than 30% of the global land area and play an important role in the Earth's system (FAO 2020; Hansen et al. 2013; IPBES 2019). Forests can absorb anthropogenic CO_2 emissions, store large carbon pools and modulate energy and water exchanges at the land–atmosphere interface (Alkama and Cescatti 2016). They are therefore considered an important mechanism for climate change mitigation (Shukla et al. 2019). However, it is reported that the forest area worldwide has declined by about 178 million ha since 1990, while the net forest loss in Africa (3.9 million ha/year) has been increasing progressively during the last three decades (FAO 2020). Such large-scale loss of forest cover reduces carbon sequestration and modifies surface energy budget and cloud formation, therefore impacts on the climate, both at regional and global scales (Bonan 2008; Wees et al. 2021).

The impact of the decline of forest cover on the regional climate is complex as the nonlinear vegetation-climate feedbacks and biogeophysical mechanisms vary in space and time. Large-scale forest cover loss generally leads to an increase of surface albedo, resulting cooling of the surface by reflecting more radiation into the atmosphere. This radiative effect is found to be dominant in temperate and boreal regions (e.g., Brovkin et al. 2006; Lee et al. 2011). On the other hand, the corresponding reduction in leaf area and stomatal resistance reduces transpiration rates, which leads to a locally warmer and drier climate, particularly in tropical rain forests (e.g., Bonan 2008; Zeng et al. 2021), but may result in more groundwater available in temperate regions (Rebelo et al. 2022). The compound effect of large-scale forest loss at different geographic locations may vary depending on which of these processes dominate (Davin and de Noblet-Ducoudré 2010; Jach et al. 2020).

Localized loss in forest cover, such as the conversion of forest to croplands and pasture, affects the energy balance and moisture cycling, and therefore the pattern and amount of precipitation (Sheil and Murdiyarso 2009; Leite-Filho et al. 2020). For example, Zeng et al. (2021) found that the recent deforestation between 2000 and 2014 over the Albertine Rift Mountains of Central Africa increased the regional warming by around 0.05°C during the dry season. Eghdami and Barros (2020) examined the implication of tropical forest loss on orographic precipitation in the eastern Andes, and found an increase in light rainfall and a decrease in moderate rainfall over the mountains. In the Amazon rainforest, Lejeune et al. (2015) performed climate simulations under projected deforestation and complete

deforestation scenarios. They found an increase of annual mean temperature of 0.5°C and a decrease of precipitation of 0.17 mm/day, and further suggested the changes reach 0.8°C and 0.22 mm/day under total deforestation. Laux et al. (2017) applied a theoretical deforestation scenario over a coastal river basin in Central Vietnam. They found that deforestation caused only marginal differences in surface energy partitioning and did not clearly affect surface air temperature and precipitation. To date, most of the modeling studies have focused on the climate impact of boreal forest loss at high latitudes and deforestation in the moist tropics, with few studies addressing regional climate change in response to forest loss in southern temperate regions, such as southern Africa.

Southern Africa is not considered to be a rich forested region, and its native forests are generally distributed in the northernmost countries located in the tropics. The Food and Agriculture Organization (FAO) reported that losses of native forest cover in southern Africa are associated with deforestation, land-use change, land degradation, forest industry activities and an increase in wildfires due to climate change (FAO 2015, 2020; Wees et al. 2021). The case of South Africa is slightly different, where tree cover has been increasing due to expanding forestry plantations, alien tree invasion and bush encroachment. Intensive commercial forestry practices, such as harvesting and planting timber plantation, have been mentioned to result in high rates of tree cover change (Curtis et al. 2018).

This study tries to fill the gap by investigating the impact of change in forest and plantation cover on local climate in southern Africa. This work is conducted within the framework of the SPACE2 joint project: South Africa Land Degradation Monitor (SALDi). Within the SALDi project, our focus is on the use of a coupled regional climate modeling approach to assess land–atmosphere interactions in the context of land degradation in southern Africa on a subcontinental scale. Land-cover changes associated with native forest loss and forestry plantations are important components of land degradation in southern Africa; therefore, its impact on regional climate is investigated in this project.

10.2 Specific Objectives

Using the WRF regional coupled land–atmosphere model, the specific objectives of this study are:

1. To evaluate the effects of two forest and plantations modified experiments on land–atmosphere interactions based on the recent stage of their cover change (2000–2015) and an extreme forest and plantation removal case in southern Africa, and
2. To quantify the general impacts of forest and plantation cover on the local and regional climate of southern Africa.

10.3   Data and Methods

10.3.1 Regional Coupled Land–Atmosphere Model

The Advanced Research version of the Weather Research and Forecast (WRF) model version 4.1 coupled with the Noah Land Surface model (LSM) is used in this case study. The WRF model (Skamarock et al. 2012) is a nonhydrostatic, fully compressible and terrain-following coordinate model developed at National Center for Atmospheric Research (NCAR). The model has been widely used for climate dynamic downscaling and regional climate impact applications. By coupling with Noah LSM, WRF is able to accurately represent interactions between the land surface and the lower atmosphere due to its physically-based model processes. To explore the land-cover changes on subgrid scales, the Noah LSM using the mosaic approach of land cover (Noah mosaic) is adopted in the study. The Noah mosaic approach (Li et al. 2013) takes into account heterogeneous land surfaces by specifying land cover with N main categories (here $N = 3$) in subgrid scale, with weightings based on the fractional coverage, instead of using the dominant land cover over each grid as in unified Noah LSM. The subgrid heterogeneity of land cover is necessary to be considered, as forest and plantation cover change is rather sporadic across the regions considered and may not modify the dominant land cover type in the whole grid cell. The Noah mosaic approach has been used in assessing the climate impact of localized deforestation in previous studies (e.g., Wang et al. 2021; Zeng et al. 2021). In the WRF model, the different effects of land cover types on land–atmosphere interactions are represented by various predetermined biogeophysical properties, specified in lookup tables, such as leaf area index, albedo, emissivity and roughness length. These will be applied in the calculation of the radiation and energy balance, as well as in the vertical transmission of moisture, heat and momentum, which further affect the temperature and moisture fields near the surface and atmospheric evolution. It should be noted that the ecological impact processes are not able to be represented in the regional coupled land–atmosphere model, and forestry plantations and native forests are treated equally in land-cover categories and in the lookup tables.

All simulations carried out in this study share the same model domain setups and physical options. The model domain has a spatial resolution of 12 km, covering the area of southern Africa (Fig. 10.1a). The model domain has 35 vertical levels with the upper boundary set to 50 hPa. The atmospheric lateral boundary conditions are provided by the Reanalysis version 5 of the European Centre for Medium-Range Weather Forecasts at a 3-hourly interval. Based on a literature review of climate dynamic downscaling applications over southern Africa (Crétat et al. 2012; Ratna et al. 2014; Ratnam et al. 2013; Zhang et al. 2023), the following model physics schemes were selected. The Betts-Miller-Janjic cumulus scheme (Janjić 1994) is used to parameterize the subgrid-scale processes of convective clouds. The WRF single-moment 6-class microphysics scheme (Hong and Lim 2006) was used to simulate the water phase exchanges in the atmosphere, and the Rapid Radiative Transfer Model for General Circulation Models (Iacono et al. 2008) is used to
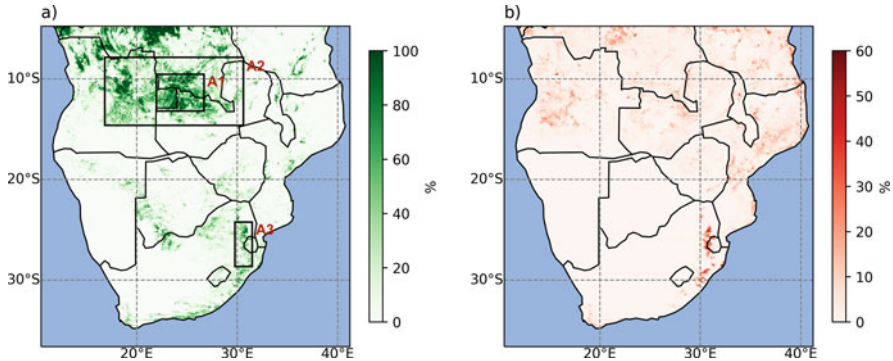
Fig. 10.1 (**a**) Forest and plantation cover over southern Africa from MODIS-derived land cover for the year 2000, and (**b**) satellite-observed forest and plantation cover loss (Hansen et al. 2013) over southern Africa between 2000 and 2015. All the datasets are aggregated to the WRF 12-km grid. The black rectangles in subplot (**a**) shows the location of the three areas for analysis (labeled A1, A2 and A3, respectively)

simulate the long-wave and short-wave radiation. The land surface turbulent fluxes are simulated by a revised Monin-Obukhov surface layer scheme (Jiménez et al. 2012), and the Yonsei University planetary boundary layer scheme (Hong et al. 2006) is used to parameterize the vertical transport concerning mass, moisture and energy fluxes transport in the planetary boundary layer.

10.3.2 Experiment Design

In order to evaluate the impact of forest and plantation cover modification on land–atmosphere interactions over southern Africa, three experiments with contrasting land-cover maps were modeled:

1. For the baseline experiment (CTL), the land-use and land-cover map from the Moderate Resolution Imaging Spectroradiometer (MODIS) 30-s product (Friedl et al. 2010) was used for representing the landscape features of the year 2000. The MODIS land-cover product provides 20 categories based on the International Geosphere-Biosphere Programme (IGBP) land-cover classifications. Those include evergreen needleleaf forest, evergreen broadleaf forest, deciduous needleleaf forest, deciduous broadleaf forest, mixed forests, closed shrublands, open shrublands, woody savannas, savannas, grasslands, permanent wetlands, croplands, urban and built up, cropland/natural vegetation mosaic, snow and ice, barren or sparsely vegetated, water, wooded tundra, mixed tundra and barren tundra.
2. The first land-cover change experiment (EXP1) represents the changed forest and plantation cover from 2000 to 2015 according to Landsat satellite observations. The forest and plantation cover change is generated from the high-resolution

global forest cover change products provided by Hansen et al. (2013), hereafter referred to as HANSEN-dataset. This dataset provides the satellite-observed forest and plantations loss as well as their gain information at a 30-m spatial resolution from the year 2000 onward. This product has been widely used in quantifying regional forest loss worldwide and has been shown to accurately capture the forest cover change in highland and lowland areas, including southern Africa (e.g., Hansen et al. 2016). To generate the forest and plantation cover map for 2015 over southern Africa, we aggregate the HANSEN-data of the forest net change, which is their forest cover gain minus forest cover loss, and then convert the total changes from the 30-m resolution to 12-km resolution in proportion to the grid cell area. Considering that the expansion of cropland is one of the main drivers of natural forest loss in Africa (FAO 2021), the conversion of forest to cropland is taken into account in the forest and plantation cover-modified land-cover map. The total change is superimposed on the forest categories in the original land-cover map of the year 2000, and an elevation threshold of 300 m a.s.l. is used to conceptually distinguish the lowland cropland and bare (sparse vegetated) ground in higher elevation area, which is similar to the approach followed in Wang et al. (2021) and Zeng et al. (2021). Cultivated land in the lowlands could be artificially irrigated and intensified throughout the year. However, crops at higher elevations are mostly rain-fed and usually sparsely vegetated during the dry season. If there is a net decrease in forest and plantation cover on a grid cell, we decrease the percentage of forest-type categories proportionately, and we treat the area as croplands if the elevation is lower than 300 m a.s.l., or we treat the area as barren or sparsely vegetated category if the elevation is above 300 m a.s.l. If there is an increase in forest and plantation cover in a grid cell, we increase the percentages of forest-type categories and decrease other land-cover categories proportionately.

3. The second forest and plantation cover change experiment (EXP2) represents an extreme scenario with a general forest and plantation cover removed, relative to the baseline (CTL). This would represent a forest loss of 100% for the tropical forest case study, and the removal of any indigenous forest and forestry plantations for the South African case study. The percentages of forest-type categories from the original MODIS land cover were converted into croplands or barren ground for all grid cells based on the above-described processes.

All three experiments (CTL, EXP1 and EXP2) use the same model configurations as described above, along with the soil texture map provided by Harmonized World Soil Database version 1.2. To isolate the impact of forest and plantation cover change-driven climate impacts, the simulations of each of the three experiments were run for the period from September 2014 to March 2015. Regarding the model spin-up period, previous studies found evidence that a one-month model spin-up period is sufficient to reach an equilibrium surface variable condition over southern Africa (e.g., Crétat et al. 2012; Ratnam et al. 2013, 2016). In this study case, we use two months as the model spin-up period, which is sufficient for the investigation. The austral summer months from November to March are chosen for analysis.

We addressed the two research objectives for three analysis areas with extensive forest and plantation cover, namely sites A1, A2 and A3 (Fig. 10.1a). Area A1 covers the northernmost part of southern Africa and has the highest native forest cover and Area A2 considers the same region but at a larger scale (and incorporates A1). Therefore, the impact of forest cover change can to some extent be explored at different scales. Forest and woodland losses have been confirmed to have occurred in sites A1 and A2 in the last decades (Mendelsohn 2019; Phiri et al. 2022). These areas are dominated by all-year-round rainfall with a hot climate. The vegetation is mainly rain-fed woody savanna/woodlands and deciduous broadleaf forests. Study site A3 is in a different climate region and biome from the last two and is located along the northern part of the Drakensberg Mountain Range, with plantation cover changes related to extensive forestry activities in this area. This area has a temperate climate and receives most of its rainfall from the Indian Ocean during the austral summer months. The cover of the plantations varies remarkably in this area and is mainly influenced by timber plantation footprint and by harvesting and planting of new rotations.

10.4   Results and Discussion

10.4.1 Validation of Model Performance

This study aims at investigating the impact of forest cover change and removal based on experimental simulation comparisons, rather than a comprehensive evaluation of the simulation results. Therefore, we validate the simulation results of the CTL experiment with observation-based high-resolution gridded datasets. The air temperature from the Climatic Research Unit (CRU) dataset (Harris et al. 2020) and the precipitation from Climate Hazards group Infrared Precipitation with Stations (CHIRPS) dataset (Funk et al. 2015) are used for validation. In order to facilitate direct comparison, the simulated temperature and precipitation are interpolated into the grids of the corresponding reference datasets. For southern Africa in the region south of 5° S, we calculate the spatial correlation from the spatial maps of values between the interpolated model results and the reference dataset.

The comparison of the spatial pattern of the averaged air temperature at 2 m above the ground is shown in Fig. 10.2. The simulation yields high spatial correlations of air temperature with the CRU dataset ($R = 0.98$, $P < 0.01$). For the monthly averaged temperature, the simulation also represents the temporal variations quite well (not shown), with slight deviations ranging from $-1.2°C$ to $0.9°C$. The results of the comparison illustrate that WRF, in general, represents the spatiotemporal variations of air temperature over southern Africa reasonably well.

In terms of precipitation, the simulation was able to replicate similar patterns compared to the reference dataset, showing the precipitation bands over the vegetated area of the northern most part of southern Africa as well as in the high mountains in the east of South Africa (Fig. 10.3). The spatial correlation coefficient between the simulation and the reference dataset is 0.76 ($P < 0.01$). However, the
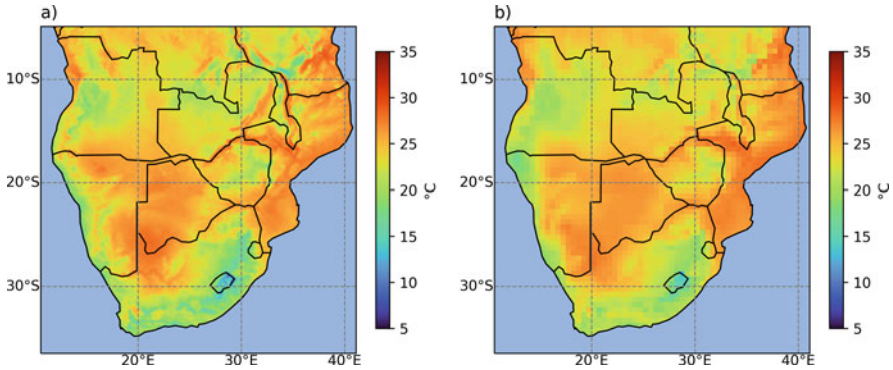
Fig. 10.2 Comparison of mean near-surface temperature between (**a**) WRF CTL simulation and (**b**) CRU dataset for the period Nov–Mar 2014/2015
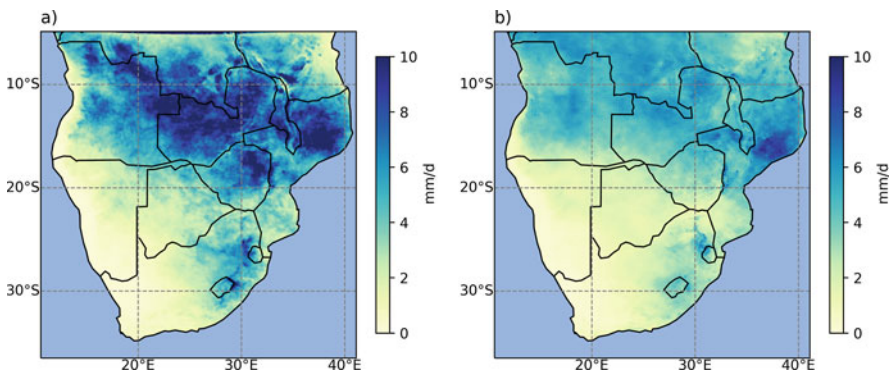

Fig. 10.3 Comparison of daily precipitation between (**a**) WRF CTL simulation and (**b**) CHRIPS dataset for the period Nov–Mar 2014/2015

simulated precipitation is generally overestimated (wet bias), which may be related to the fact that grided precipitation data usually underestimate precipitation over complex terrain area. Specific to the three analysis areas, the overestimation of precipitation reaches up to 40%. Nevertheless, such wet biases are often reported in precipitation simulation by dynamic downscaling models (e.g., Crétat et al. 2012; Ratna et al. 2014; Ratnam et al. 2012).

10.4.2 Impacts of Current Forest and Plantation Cover Change on Regional Climate and Land–Atmosphere Interactions

In EXP1, the change in forest and plantation cover is mainly reflected by a slight modification of percentage value in forest-type in the land-cover map. This forest and plantation cover change was found to modify the local precipitation
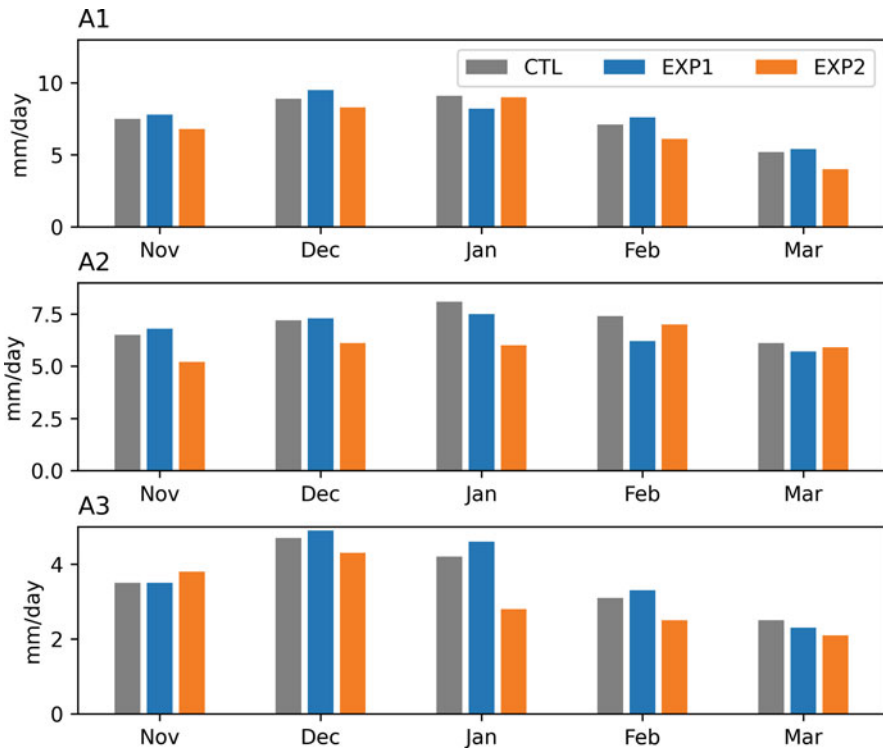
Fig. 10.4 Simulated monthly precipitation (mm/d) for the three experiments (CTL, EXP1 and EXP2) averaged over the analysis area shown in Fig. 10.1a, in southern Africa

only slightly. The monthly precipitation in the three analysis areas has changed moderately by about 1 mm/day (Fig. 10.4). The surface soil moisture content in EXP1 only marginally differs from the CTL (Fig. 10.5). Moreover, the standard deviations have similar values, indicating a comparable daily variation in soil moisture between CTL and EXP1.

Figure 10.6 illustrates the derived diurnal cycle of air temperature, sensible heat flux, latent heat flux and specific humidity for three analysis areas. All these surface variables show similar diurnal variations for CTL and EXP1 (Fig. 10.6). Some differences can be identified, including a slight increase in daytime air temperature and sensible heat flux, and a decrease in latent heat and specific humidity. These effects are comparatively small, because the changes in land cover are resolved at the subgrid scale in the WRF simulations, small percentage change in land-cover types very slightly influence the land–atmosphere coupling strength. Nevertheless, using the WRF Noah Mosaic approach, the forest and plantation cover change during the period 2000–2015 is simulated to be able to produce potential climate impacts in southern Africa.
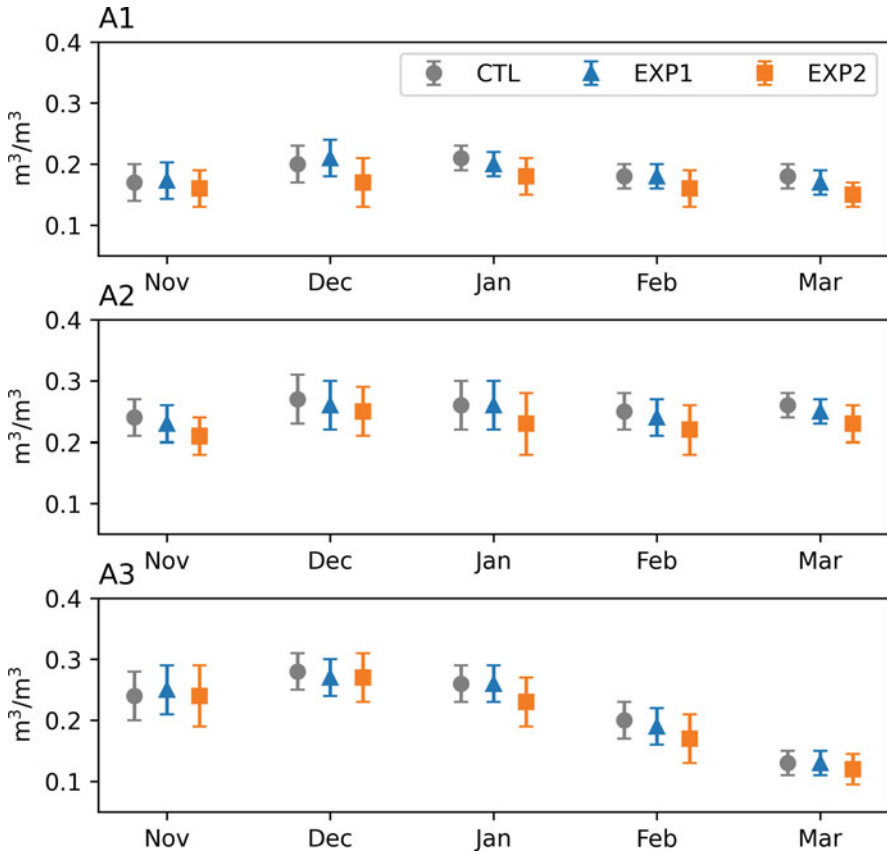
Fig. 10.5 Simulated mean surface soil moisture content for the three experiments (CTL, EXP1 and EXP2) for the three analysis areas shown in Fig. 10.1a, in southern Africa. The whiskers depict the standard deviation

10.4.3 Potential Impacts of Forest and Plantation Removal on Land–Atmosphere Interactions

The simulated total removal of forest and plantation removal experiment (EXP2) was found to have a remarkable impact on surface variables. In most cases, EXP2 exhibits a lower precipitation than CTL and EXP1 (Fig. 10.4). The surface soil moisture in EXP2 is generally lower than CTL in all three analysis areas due to the loss of the forest and plantation cover (Fig. 10.5), despite the variations of precipitation. It is evident that the standard deviation of soil moisture in EXP2 is larger than that of CTL and EXP1, indicating that the canopy interception of precipitation by forest and plantations reduces the soil moisture variations relative to bare ground and crop cover.
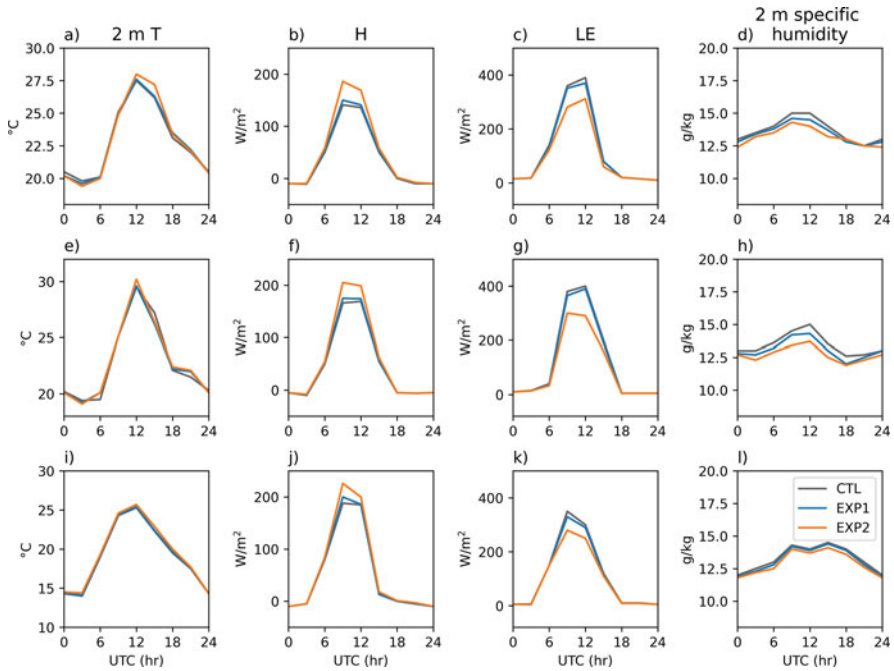
Fig. 10.6 Diurnal cycle of simulated 2 m temperature (first column), sensible heat flux H (second column), latent heat flux LE (third column), and 2 m specific humidity (fourth column) for the three experiments (CTL, EXP1 and EXP2) averaged over the three analysis areas A1 (top row), A2 (middle row) and A3 (bottom row) in southern Africa, respectively. The *x*-axis represents the hour in UTC time

As shown in Fig. 10.6, the daytime air temperature in EXP2 is marginally higher than that in CTL and EXP1. The removal of forest and plantations increases the temperature around 0.3 to 0.6°C at the diurnal peaks for three study sites. This higher air temperature is associated with increased sensible heat flux, decreased latent heat flux and decreased specific humidity during the daytime. This is attributed to the fact that transpiration and canopy evaporation are greatly reduced following the entire transfer of forest and plantation cover to croplands and barren ground. Moreover, even though the removal of forest and plantation cover can enhance the evaporation capacity of the soil, the overall evapotranspiration is still reduced, due to the fact that the water availability over southern Africa is mostly insufficient and depends mainly on rainfall. Overall, our modeling results that the total loss of forest and plantation cover could result in a warmer and drier local climate. It is worth noting that, for the three study regions with their different sizes, the above impacts on land–atmosphere interactions are consistent to a large degree.

The precipitation recycling ratio (PRR), defined as the contribution of the evaporated water to the precipitation within the same region, is a commonly used measure for quantifying land–atmosphere interactions (i.e., Arnault et al. 2016;

Fig. 10.7 Calculated
monthly precipitation
recycling ratio (PRR) for area
A2, in the northmost region
of southern Africa
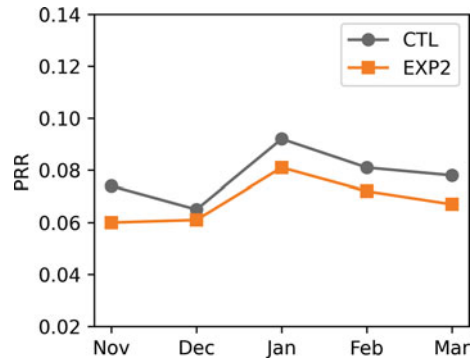
Zhang et al. 2019). For a specific region, a higher PRR value corresponds to more evaporated water contributing to the local precipitation (Zhang et al. 2022). Here we calculate monthly PRR values following the method of Schär et al. (1999). Since the analytical calculation of water recycling is strongly dependent on the shape and size of the area (e.g., Rios-Entenza and Miguez-Macho 2014; Trenberth 1999), this PRR value is calculated only for the large area A2. The PRR values computed for the experiments CTL and EXP2 are shown in Fig. 10.7. The results show that the overall PRR values of area A2 are 6.9% and 7.8% for CTL and EXP2, respectively. Moreover, for all months, PRR values in EXP2 are smaller than the values in CTL, which indicates that the simulation of the removal of forest and plantation cover reduces the local water recycling. This result is supportive to the knowledge that large extent of forest cover contributes to positive feedbacks to the precipitation, i.e., more forest cover increases the evapotranspiration and the local precipitation.

Although studies have shown that increased surface albedo associated with deforestation cools the surface and may mitigate climate warming in some regions (Lee et al. 2011; Williams et al. 2021), our findings suggest that the decrease in forest and plantation cover in southern Africa may lead to a warmer and drier local climate during the rainy austral summer. This may be related to the very strong evaporative capacity (e.g., the potential evapotranspiration) in southern Africa (Trabucco and Zomer 2019). It is worth noting that the drier and warmer effect may accumulate over the years, due to the long-term memory of soil moisture and the identified positive feedback on precipitation.

10.5   Summary and Outlook

In this study, we addressed the potential impact of forest and plantation cover change on regional climate and land–atmosphere interactions over southern Africa. Regional coupled land–atmosphere WRF model simulations were performed, with the different extent of forest-type categories prescribed as the land surface boundary. Based on the results presented above, it is concluded that the extreme experiment of the removal of forest cover in southern Africa may result in a warmer and drier

climate during the austral summer months. The local precipitation recycling ratio was simulated have notably decreased due to the removal of forest cover, suggesting that forest and plantation positively contribute to local precipitation. Although the model results are affected by noise (internal model variabilities), our results for different sized areas and with different extents of forest and plantation cover change give sufficient evidence for conclusions.

Our results suggest that decision- and policymakers should focus attention on sustainable land management strategies to reduce the loss of native forests and properly manage forestry plantations for climate change mitigation. As southern Africa is not rich in forest resources, preserving what remains of the original and native forests is particularly important. Using established nature conservation areas to protect forest resources should be one of the most effective method. Since the major drivers of local deforestation in Africa include agriculture and cutting trees for firewood, preventative measures could include sustainable and appropriate population growth, the development of sustainable agriculture, as well as the use of renewable energy. Of course, robust policy interventions need to joint consideration of human and ecological sustainability and development and the related trade-offs. Governments and nongovernmental organizations should take the initiative to develop vigorous ecosystem restoration plans to re-establish forests and put long-term sustainability ahead of short-term concerns, which can be most effective in adapting to climate change.

This study provides a first step toward analyzing how forest and plantation modification affects the land–atmosphere interactions over southern Africa. A limitation of this study is that the aggregation of the change in forest cover into the coupled land–atmosphere model at mesoscale grid prevents many land surface characteristics from being properly represented. The imperfect classification of land-cover categories and the lookup table values assigned for land surface modeling lead to additional uncertainties in WRF simulations. Indeed, the nondistinction between native forests and forestry plantations, and the lack of consideration of ecological processes limit the model ability to simulate the potential role of forest and plantations in climate change in more detail. A fine spatial model resolution (< 4 km) would be beneficial for further investigation of the climate impact of forest and plantation cover change at convective scale and for extreme rainfall events. In particular, when combining in-situ measurements with very high-resolution modeling (< 1 km) for specific hotspot areas, the microclimate impact by forest and plantations can be investigated in more depth. Additionally, long-term model simulations and considering model internal uncertainties would allow an even deeper analysis.

References

Alkama R, Cescatti A (2016) Biophysical climate impacts of recent changes in global forest cover. Science 351(6273):600–604. https://doi.org/10.1126/science.aac8083

Arnault J, Knoche R, Wei J, Kunstmann H (2016) Evaporation tagging and atmospheric water budget analysis with WRF: A regional precipitation recycling study for West Africa. Water Resour Res 52(3):1544–1567. https://doi.org/10.1002/2015WR017704

Bonan GB (2008) Forests and climate change: Forcings, feedbacks, and the climate benefits of forests. Science 320(5882):1444–1449. https://doi.org/10.1126/science.1155121

Brovkin V, Claussen M, Driesschaert E, Fichefet T, Kicklighter D, Loutre MF, Matthews HD, Ramankutty N, Schaeffer M, Sokolov A (2006) Biogeophysical effects of historical land cover changes simulated by six Earth system models of intermediate complexity. Clim Dyn 26(6):587–600. https://doi.org/10.1007/s00382-005-0092-6

Crétat J, Pohl B, Richard Y, Drobinski P (2012) Uncertainties in simulating regional climate of Southern Africa: sensitivity to physical parameterizations using WRF. Clim Dyn 38(3–4):613–634. https://doi.org/10.1007/s00382-011-1055-8

Curtis PG, Slay CM, Harris NL, Tyukavina A, Hansen MC (2018) Classifying drivers of global forest loss. Science 361(6407):1108–1111. https://doi.org/10.1126/science.aau3445

Davin EL, de Noblet-Ducoudré N (2010) Climatic impact of global-scale deforestation: radiative versus nonradiative processes. J Clim 23(1):97–112. https://doi.org/10.1175/2009JCLI3102.1

Eghdami M, Barros AP (2020) Deforestation impacts on orographic precipitation in the tropical Andes. Front Environ Sci 8(November):1–14. https://doi.org/10.3389/fenvs.2020.580159

FAO (2015) Southern Africa's forests and people. FAO, Rome

FAO (2020) Global forest resources assessment 2020 – key findings. FAO, Rome. https://doi.org/10.4060/ca8753en

FAO (2021) Global forest resources assessment 2020 – Remote sensing survey. FAO, Rome. https://www.fao.org/forest-resources-assessment/remote-sensing/fra-2020-remote-sensing-survey/en/

Friedl MA, Sulla-Menashe D, Tan B, Schneider A, Ramankutty N, Sibley A, Huang X (2010) MODIS collection 5 global land cover: algorithm refinements and characterization of new datasets. Remote Sens Environ 114(1):168–182. https://doi.org/10.1016/j.rse.2009.08.016

Funk C, Peterson P, Landsfeld M, Pedreros D, Verdin J, Shukla S, Husak G, Rowland J, Harrison L, Hoell A, Michaelsen J (2015) The climate hazards infrared precipitation with stations—a new environmental record for monitoring extremes. Sci Data 2(1):150066. https://doi.org/10.1038/sdata.2015.66

Hansen MC, Potapov PV, Moore R, Hancher M, Turubanova SA, Tyukavina A, Thau D, Stehman SV, Goetz SJ, Loveland TR, Kommareddy A, Egorov A, Chini L, Justice CO, Townshend JRG (2013) High-resolution global maps of 21st-century forest cover change. Science 342(6160):850–853. https://doi.org/10.1126/science.1244693

Hansen MC, Potapov PV, Goetz SJ, Turubanova S, Tyukavina A, Krylov A, Kommareddy A, Egorov A (2016) Mapping tree height distributions in Sub-Saharan Africa using Landsat 7 and 8 data. Remote Sens Environ 185:221–232. https://doi.org/10.1016/j.rse.2016.02.023

Harris I, Osborn TJ, Jones P, Lister D (2020) Version 4 of the CRU TS monthly high-resolution gridded multivariate climate dataset. Sci Data 7(1):109. https://doi.org/10.1038/s41597-020-0453-3

Hong S-Y, Lim JJ (2006) The WRF single-moment 6-class microphysics scheme (WSM6). Asia-Pac J Atmos Sci 42:129–151

Hong S-Y, Noh Y, Dudhia J (2006) A new vertical diffusion package with an explicit treatment of entrainment processes. Mon Weather Rev 134(9):2318–2341. https://doi.org/10.1175/MWR3199.1

Iacono MJ, Delamere JS, Mlawer EJ, Shephard MW, Clough SA, Collins WD (2008) Radiative forcing by long-lived greenhouse gases: calculations with the AER radiative transfer models. J Geophys Res 113(D13):D13103. https://doi.org/10.1029/2008JD009944

IPBES. (2019). Global assessment report on biodiversity and ecosystem services of the inter-governmental science-policy platform on biodiversity and ecosystem services. https://doi.org/10.5281/ZENODO.5517154

Jach L, Warrach-Sagi K, Ingwersen J, Kaas E, Wulfmeyer V (2020) Land cover impacts on land-atmosphere coupling strength in climate simulations with WRF over Europe. J Geophys Res Atmos 125(18). https://doi.org/10.1029/2019JD031989

Janjić ZI (1994) The step-mountain eta coordinate model: further developments of the convection, viscous sublayer, and turbulence closure schemes. Mon Weather Rev 122(5):927–945. https://doi.org/10.1175/1520-0493(1994)122<0927:TSMECM>2.0.CO;2

Jiménez PA, Dudhia J, González-Rouco JF, Navarro J, Montávez JP, García-Bustamante E (2012) A revised scheme for the WRF surface layer formulation. Mon Weather Rev 140(3):898–918. https://doi.org/10.1175/MWR-D-11-00056.1

Laux P, Nguyen PNB, Cullmann J, Van TP, Kunstmann H (2017) How many RCM ensemble members provide confidence in the impact of land-use land cover change? Int J Climatol 37:2080–2100. https://doi.org/10.1002/joc.4836

Lee X, Goulden ML, Hollinger DY, Barr A, Black TA, Bohrer G, Bracho R, Drake B, Goldstein A, Gu L, Katul G, Kolb T, Law BE, Margolis H, Meyers T, Monson R, Munger W, Oren R, Paw UKT, Richardson AD, Schmid HP, Staebler R, Wofsy S, Zhao L (2011) Observed increase in local cooling effect of deforestation at higher latitudes. Nature 479(7373):384–387. https://doi.org/10.1038/nature10588

Leite-Filho AT, Costa MH, Fu R (2020) The southern Amazon rainy season: the role of deforestation and its interactions with large-scale mechanisms. Int J Climatol 40(4):2328–2341. https://doi.org/10.1002/joc.6335

Lejeune Q, Davin EL, Guillod BP, Seneviratne SI (2015) Influence of Amazonian deforestation on the future evolution of regional surface fluxes, circulation, surface temperature and precipitation. Clim Dyn 44(9–10):2769–2786. https://doi.org/10.1007/s00382-014-2203-8

Li D, Bou-Zeid E, Barlage M, Chen F, Smith JA (2013) Development and evaluation of a mosaic approach in the WRF-Noah framework. J Geophys Res Atmos 118(21):11,918–11,935. https://doi.org/10.1002/2013JD020657

Mendelsohn JM (2019) Landscape changes in Angola. In: Huntley B, Russo V, Lages F, Ferrand N (eds) Biodiversity of Angola. Springer, Cham. https://doi.org/10.1007/978-3-030-03083-4_8

Phiri D, Chanda C, Nyirenda VR, Lwali CA (2022) An assessment of forest loss and its drivers in protected areas on the Copperbelt province of Zambia: 1972–2016. Geomat Nat Haz Risk 13(1):148–166. https://doi.org/10.1080/19475705.2021.2017021

Ratna SB, Ratnam JV, Behera SK, Rautenbach CJ d W, Ndarana T, Takahashi K, Yamagata T (2014) Performance assessment of three convective parameterization schemes in WRF for downscaling summer rainfall over South Africa. Clim Dyn 42(11–12):2931–2953. https://doi.org/10.1007/s00382-013-1918-2

Ratnam JV, Behera SK, Masumoto Y, Takahashi K, Yamagata T (2012) A simple regional coupled model experiment for summer-time climate simulation over southern Africa. Clim Dyn 39(9–10):2207–2217. https://doi.org/10.1007/s00382-011-1190-2

Ratnam JV, Behera SK, Ratna SB, de Rautenbach CJW, Lennard C, Luo JJ, Masumoto Y, Takahashi K, Yamagata T (2013) Dynamical downscaling of austral summer climate forecasts over Southern Africa using a regional coupled model. J Clim 26(16):6015–6032. https://doi.org/10.1175/JCLI-D-12-00645.1

Ratnam JV, Behera SK, Doi T, Ratna SB, Landman WA (2016) Improvements to the WRF seasonal hindcasts over South Africa by bias correcting the driving sintex-F2v CGCM fields. J Clim 29(8):2815–2829. https://doi.org/10.1175/JCLI-D-15-0435.1

Rebelo AJ, Holden PB, Hallowes J, Eady B, Cullis J, Esler KJ, New MG (2022) The hydrological impacts of restoration: A modelling study of alien tree clearing in four mountain catchments in South Africa. J Hydrol 127771:127771

Rios-Entenza A, Miguez-Macho G (2014) Moisture recycling and the maximum of precipitation in spring in the Iberian Peninsula. Clim Dyn 42(11–12):3207–3231. https://doi.org/10.1007/s00382-013-1971-x

Schär C, Lüthi D, Beyerle U, Heise E (1999) The soil–precipitation feedback: a process study with a regional climate model. J Clim 12(3):722–741. https://doi.org/10.1175/1520-0442(1999)012<0722:TSPFAP>2.0.CO;2

Sheil D, Murdiyarso D (2009) How forests attract rain: an examination of a new hypothesis. Bioscience 59(4):341–347. https://doi.org/10.1525/bio.2009.59.4.12

Shukla PR, Skea J, Calvo Buendia E, Masson-Delmotte V, Pörtner HO, Roberts DC, Zhai P, Slade R, Connors S, van Diemen R (2019) IPCC, 2019: climate change and land: an IPCC special report on climate change, desertification, land degradation, sustainable land management, food security, and greenhouse gas fluxes in terrestrial ecosystems. IPCC, Geneva

Skamarock WC, Klemp JB, Duda MG, Fowler LD, Park S-H, Ringler TD (2012) A multiscale nonhydrostatic atmospheric model using Centroidal Voronoi Tesselations and C-grid staggering. Mon Weather Rev 140(9):3090–3105. https://doi.org/10.1175/MWR-D-11-00215.1

Trabucco A, Zomer R (2019) Global aridity index and potential evapotranspiration (ET0) climate database v2. Figshare Dataset. https://doi.org/10.6084/m9.figshare.7504448.v3

Trenberth KE (1999) Atmospheric moisture recycling: role of advection and local evaporation. J Clim 12(5 II):1368–1381. https://doi.org/10.1175/1520-0442(1999)012<1368:amrroa>2.0.co;2

Wang D, Wu J, Huang M, Li LZX, Wang D, Lin T, Dong L, Li Q, Yang L, Zeng Z (2021) The critical effect of subgrid-scale scheme on simulating the climate impacts of deforestation. J Geophys Res Atmos 126:1–12. https://doi.org/10.1029/2021jd035133

Wees D, Werf GR, Randerson JT, Andela N, Chen Y, Morton DC (2021) The role of fire in global forest loss dynamics. Glob Chang Biol 27(11):2377–2391. https://doi.org/10.1111/gcb.15591

Williams CA, Gu H, Jiao T (2021) Climate impacts of U.S. forest loss span net warming to net cooling. Sci Adv 7(7). https://doi.org/10.1126/sciadv.aax8859

Zeng Z, Wang D, Yang L, Wu J, Ziegler AD, Liu M, Ciais P, Searchinger TD, Yang Z, Chen D, Chen A, Li LZX, Piao S, Taylor D, Cai X, Pan M, Peng L, Lin P, Gower D et al (2021) Deforestation-induced warming over tropical mountain regions regulated by elevation. Nat Geosci 14(1):23–29. https://doi.org/10.1038/s41561-020-00666-0

Zhang Z, Arnault J, Wagner S, Laux P, Kunstmann H (2019) Impact of lateral terrestrial water flow on land-atmosphere interactions in the Heihe River basin in China: fully coupled modeling and precipitation recycling analysis. J Geophys Res Atmos 124(15):8401–8423. https://doi.org/10.1029/2018JD030174

Zhang Z, Arnault J, Laux P, Ma N, Wei J, Shang S, Kunstmann H (2022) Convection-permitting fully coupled WRF-Hydro ensemble simulations in high mountain environment: impact of boundary layer- and lateral flow parameterizations on land-atmosphere interactions. Clim Dyn 59(5-6):1355–1376. https://doi.org/10.1007/s00382-021-06044-9

Zhang Z, Laux P, Baade J, Arnault J, Wei J, Wang X, Liu Y, Schmullius C, Kunstmann H (2023) Impact of alternative soil data sources on the uncertainties in simulated land-atmosphere interactions. Agri For Meteorol 339(March):109565. https://doi.org/10.1016/j.agrformet.2023.109565